PAPER Nr. : 21

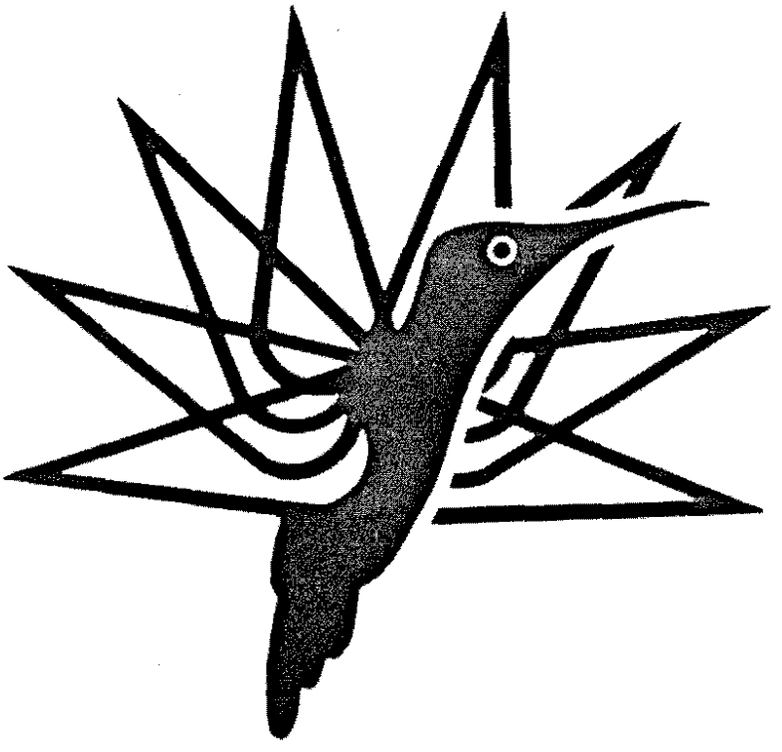

DESIGN OF THE 225-KNOT CONVENTIONAL ROTOR

Francis J. McHugh
Boeing Vertol Company
Philadelphia, Pennsylvania
USA

TENTH EUROPEAN ROTORCRAFT FORUM

AUGUST 28 – 31, 1984 – THE HAGUE, THE NETHERLANDS

DESIGN OF THE 225-KNOT CONVENTIONAL ROTOR

Francis J. McHugh
Boeing Vertol Company
Philadelphia, Pennsylvania

1. ABSTRACT

During the mid-1970's, testing and analytical studies were conducted to develop a better understanding of the characteristics and limitations of the conventional rotor at forward speeds beyond 200 knots. The increased understanding and improved mathematical modeling of the rotor in the high-speed regime formed a basis for designing the next-generation rotor system with a maximum cruise efficiency (L/De) speed of 180 knots and a maximum cruise speed of 200 knots. A series of models was built and tested to demonstrate the design objectives of this high-speed rotor. Model test results indicated maximum cruise efficiency (L/De) at 180 knots and capability up to 231 knots.

The next stage in the continued development of the conventional rotor is to define an advanced rotor that will have a design cruise speed of 225 knots for maximum cruise efficiency. The design approach for this rotor is to minimize induced and profile power at 225 knots, thereby achieving maximum lift to equivalent drag (L/De). A summary of the design approach will be presented with the change in rotor L/De as the design process moves from an ideal rotor to a realistic design. A few sensitivities will be included that lead to the performance of the final configuration.

2. NOTATION

GW = aircraft gross weight, lb

L = rotor lift, lb

d = rotor diameter, ft

De = equivalent rotor drag, lb

fe = equivalent flat-plate drag, ft^2

M_{DD} = drag divergence Mach number, nd

$M_{1,90}$ = advancing-tip Mach number, nd

P = rotor power, hp

q = dynamic pressure, $\rho V^2/2$ lb/ft^2

r = rotor radius, ft

T = rotor thrust, lb

V = forward flight speed, ft/sec

V_T = rotor tip speed, ft/sec

X = rotor propulsive force, lb

$C_{l_{max}}$ = maximum section lift coefficient, nd

C_P = rotor power coefficient, $P/\rho\pi r^2 V_T^3$

C_T = rotor lift coefficient, $T/\rho\pi r^2 V_T^2$

$\overline{X}$ = rotor propulsive force coefficient, $X/qd^2\sigma$

μ = advance ratio, V/V_T

ρ = density of air, lb sec ^{2}/ft^4

π = Pi, nd

σ = rotor solidity, $bc/\pi r$, nd

3. INTRODUCTION

Exploratory testing in the mid-1970's, documented in Reference 1, indicated that the conventional helicopter rotor had the capability to operate in the high-speed regime (advance ratios up to 0.60). This led to the testing summarized in Reference 2 to determine if there were any lift or propulsive force limits in the high-speed regime. There were no propulsive force limits. The limits to lift were aerodynamic, not model structural or aeroelastic limits, and resulted in a reduction in lift with an increase in collective pitch, indicating severe rotor stall. With the demonstration of rotor operation in the lifting and propelling mode at speeds up to 225 knots, Boeing Vertol continued their development of the conventional rotor in the high-speed regime with increased emphasis. A rotor development program was initiated to define airfoils and a rotor that would maximize performance at 180 knots. The results of this rotor development produced a rotor with a full-scale rotor lift-to-equivalent drag ratio (L/De) of approximately 10 at 180 knots and are summarized in Reference 3.

Based on the potential indicated by these rotor test programs, we initiated a study to determine the design speed for the next-generation rotor system. We started with The 1985 Commercial Transport Study that was performed for NASA in the early 1970's. It was upgraded, incorporating the improved level of rotor performance projected from the high-speed test data, to examine the impact on cost of flat-plate area drag loading (gross weight to flat-plate drag area ratio, GW/fe) and design speed. The parameter that measures the overall performance of a commercial transport is direct operating cost (DOC). Figure 1 presents the DOC as influenced by drag loadings from GW/fe = 700 lb/ft^2 to GW/fe = 3,000 lb/ft^2, corresponding to aerodynamically dirty or very clean aircraft. The forward flight speed range examined was 160 to 250 knots and is compatible with the aerodynamic cleanliness range. As indicated in Figure 1, there

is a minimum in DOC for each speed. The trend through these minimums defines the most cost-efficient configurations. From reviews of test data, reports, and papers in the area of drag of advanced configurations, it is evident that a drag loading of 1,500 lb/ft^2 would be a desirable goal and would require careful development to achieve. This drag loading and minimum DOC specify the speed at 225 knots, an increase of 45 knots over the 180-knot rotor recently developed that was 45 knots over the speed for maximum L/De of the Chinook (CH-47D). Both the drag loading and speed have been selected as goals that must be worked aggressively to achieve. These study results, in addition to the high-speed rotor testing, were encouraging enough to obtain support from NASA for performing a study to define a rotor system designed to maximize performance at 225 knots. This program, "Study of Advanced Flight Research Rotor," contract NAS2-10826, was conducted under the cognizance of Leonard Haslim, the technical monitor, and is the subject of this paper.

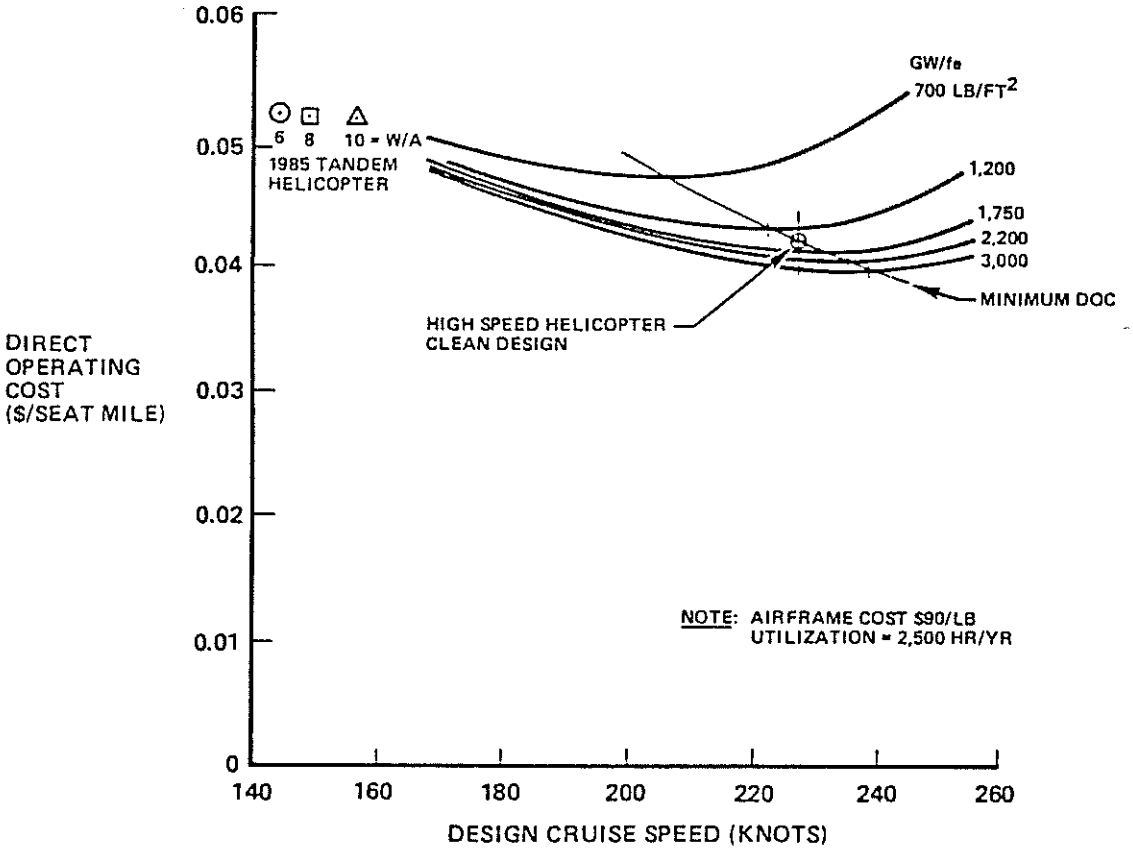

Figure 1. Impact of Design Cruise Speed and Drag Loading on Direct Operating Cost

4. BACKGROUND

The objective of the NASA program was to define a rotor that would achieve a maximum reduction in forward flight power required at 225 knots. The approach was to examine the variation of rotor performance to geometry variations and provide a baseline rotor definition, develop the sensitivity of the baseline to selected configuration modifications, and then conduct a preliminary design. The emphasis of this paper will be on the baseline rotor definition studies accomplished, with a few details on the sensitivity study results and the preliminary design.

5. GROUND RULES

With a demonstrated capability to operate in the high-speed regime, the conventional rotor that provides the lift and propulsive force for the aircraft was selected as the candidate for the advanced flight research rotor (AFRR). It does not incorporate any segments, independently controlled blade sections, or flaps. It does include planform taper, twist, sweep, and structural tuning as required to improve the performance, blade loads, and hub loads. The AFRR can incorporate higher harmonic pitch for further improvements.

The study ground rules that were initially established to define a rotor in the high-speed cruise regime specified a forward speed of 225 knots and a drag loading of 1,500 lb/ft^2. The rotor will have four blades and will incorporate advanced airfoils developed by Boeing Vertol for operation at high speed. The VR-12 airfoil is the working section to be used from the blade root to the 85-percent blade radial station and will taper linearly to the VR-15 airfoil at the rotor tip. These airfoils were developed to maximize lift (Cl_{max}) at Mach 0.40 and maximize the drag divergence Mach number at zero lift, while maintaining high lift between these two design conditions. An extensive amount of wind tunnel testing has been performed to substantiate their characteristics. To establish the level of improvement achieved by these airfoils, a comparison with the characteristics of other airfoils at the design conditions is presented in Figure 2. The lower line is for the VR-7/8 family that was developed to minimize drag in hover and low forward speed for the Heavy-Lift Helicopter; the VR-9 was developed for the YUH-61 UTTAS aircraft. The next band moving up the figure represents the latter-day airfoils such as the NASA supercritical and the NLR-1. The top band in Figure 2 is the VR-12/15 family which shows a significant improvement over the other airfoils in terms of increased maximum lift or drag divergence Mach number.

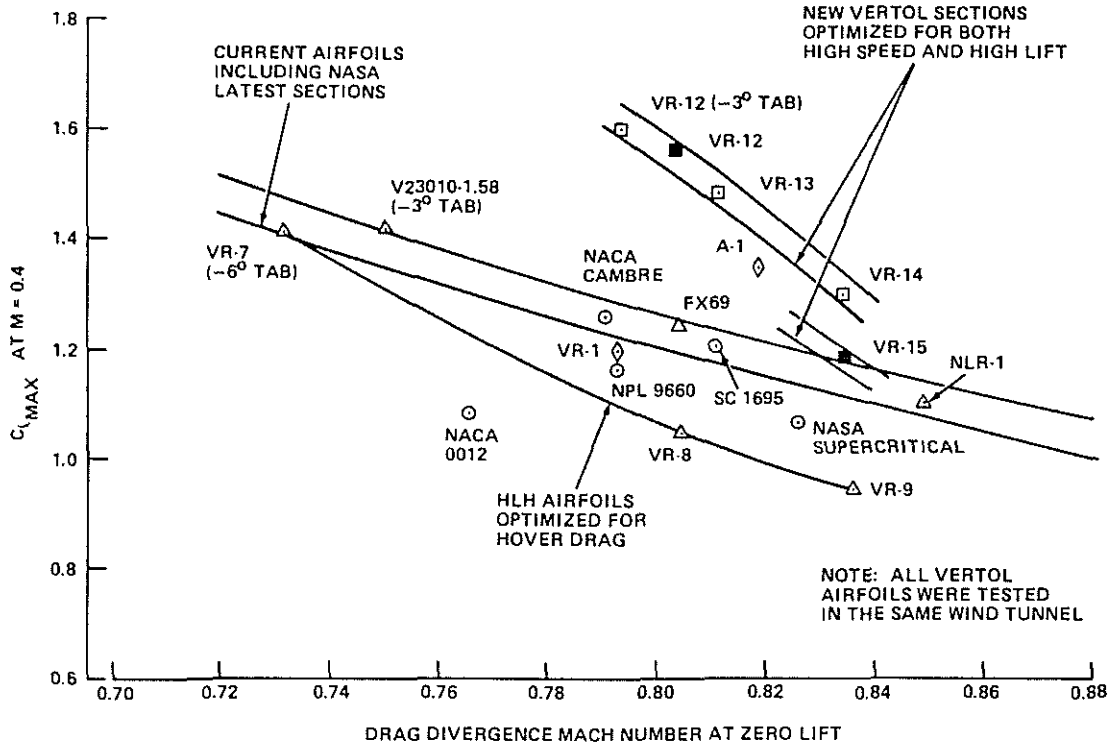

Figure 2. Comparison of Airfoil Characteristics at Design Conditions

An advancing-tip Mach number limit of 0.90 was selected as a design ground rule for the AFRR. From the testing presented in Reference 3, performance was compared for a number of rotors at a fixed advance ratio (μ), rotor lift coefficient (CT/σ), and rotor propulsive force coefficient ($\overline{X}$) in Figure 3. Shown is rotor power coefficient (C_P/σ) for a model CH-47D rotor with VR-7/8 airfoils compared to a model of the Boeing Vertol Model 360 rotor with VR-12/15 airfoils. At low Mach numbers there is no difference between the rotors, but beyond a Mach number of 0.86 the rotor with VR-7/8 airfoils shows an increase in power that becomes significant at 0.90 Mach number while there is no increase in rotor power coefficient at Mach numbers of 0.91 for the rotor with VR-12/15 airfoils.

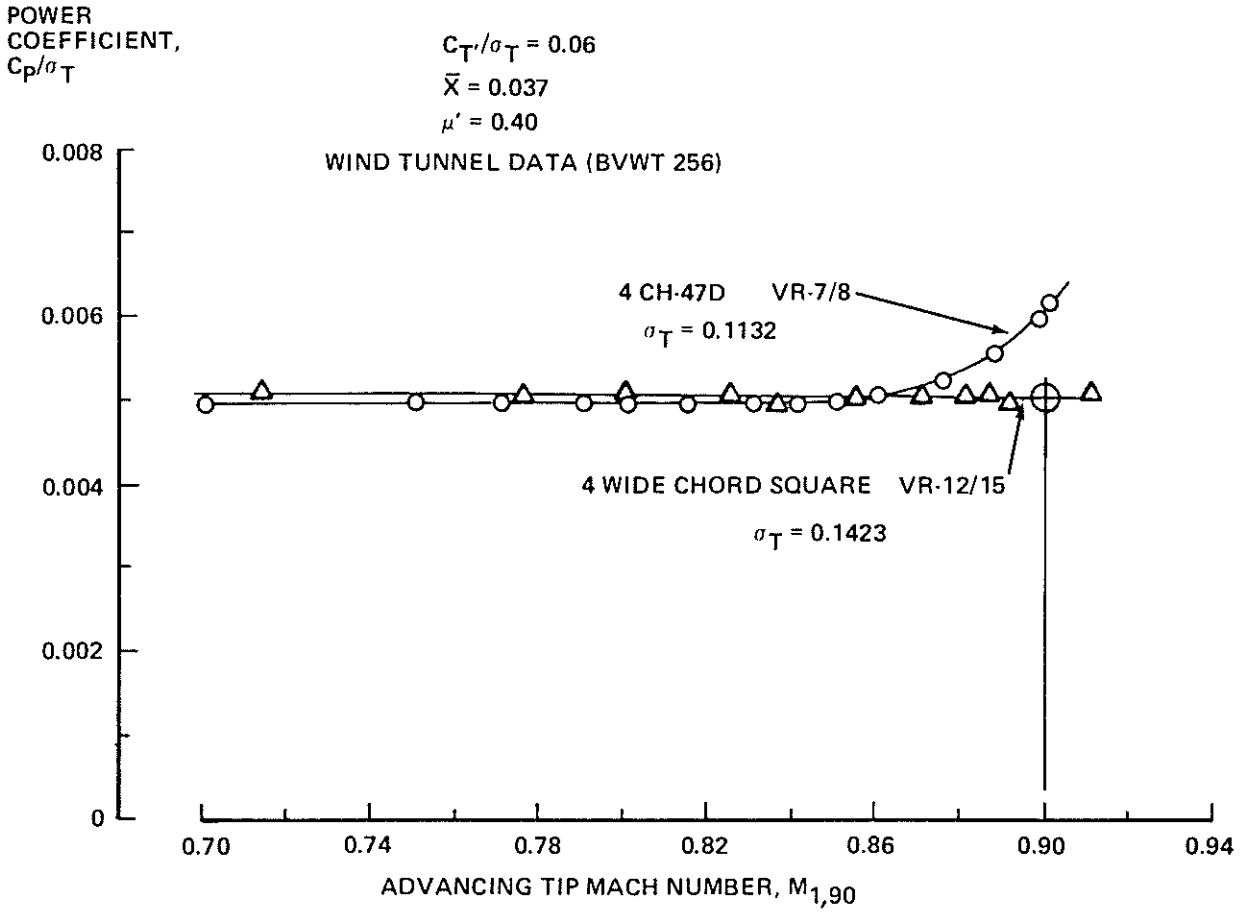

Figure 3. Performance Improvement From Reduced Compressibility

The next ground rule to be defined is the rotor disk loading. An examination of the historical trend of drag loading with gross weight shown in Figure 4 indicates that a gross weight of 25,000 pounds is consistent with an aircraft that is considered a clean design and has a drag loading of 1,500 lb/ft^2. This gross weight and the historical trends of rotor disk loading and gross weight for single- and tandem-rotor helicopters as shown in Figure 5 define a disk loading of 6.25 lb/ft^2 for a tandem-rotor helicopter. This results in a 51-foot-diameter rotor, which is the same size as the CH-46 rotor. The CH-46 rotor will be used as the reference rotor for this study and will aid in the definition of the magnitude of the performance improvement.

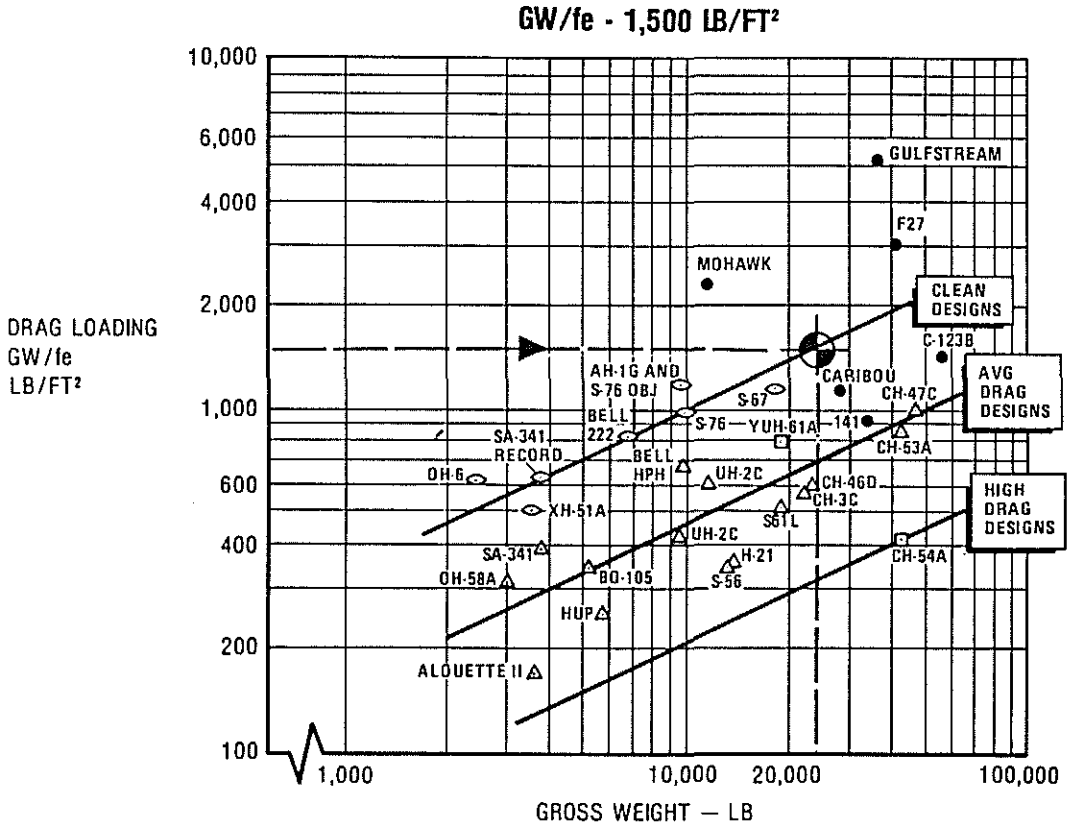

Figure 4. Historical Trends of Drag Loading and Gross Weight

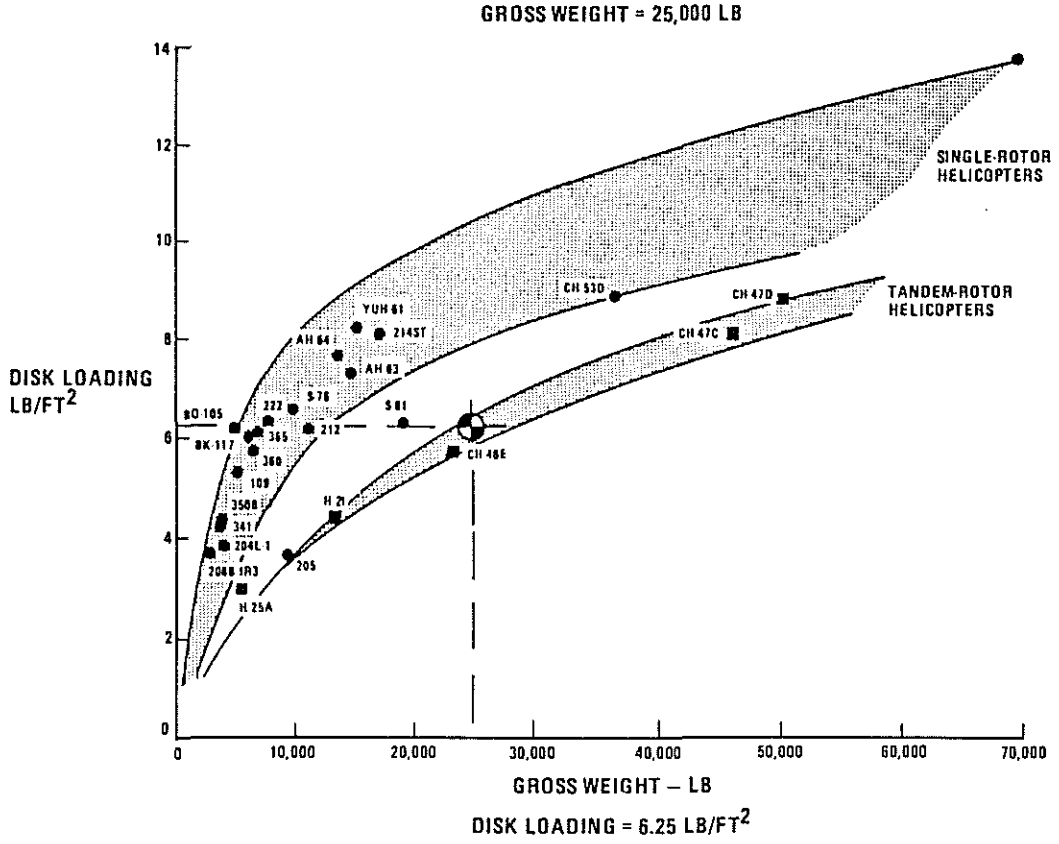

Figure 5. Historical Trends of Disk Loading and Gross Weight

6. APPROACH

The basic portion of this study is the conceptual study. It is divided into four areas:

1. The preliminary study will establish the optimum blade planform, elastic twist, and control based on the aerodynamic performance considerations.

2. The parametric study will review tradeoffs to evaluate methods for tailoring the elastic twist.

3. The selection of the baseline.

4. The feasibility study will determine the relative feasibility of achieving this design.

The scope of the preliminary study was to establish blade planform and elastic twist based on maximizing aerodynamic performance. The first task was to define an ideal rotor in which each radial and azimuthal element is operated at the angle of attack for maximum lift-to-drag ratio for the section and to minimize profile power. It is also desirable to have a loading distribution that will produce approximately uniform downwash in the far wake and minimize induced power. This would result in the blade chord as well as the angle of attack varying at each radial and azimuth and would be represented by a rotor that had a "rubber chord and rubber twist" and is the ideal, a goal to be achieved. Applied to this goal will be a series of constraints that eventually result in a real rotor. The first step is to constrain the chord so it does not vary around the azimuth for each radial bay and is designated the optimum rotor. The planform could have taper, inverse taper, or whatever is required. The next step would be to constrain each blade radial station pitch to the steady plus the first five harmonics so the optimum rotor has a fixed radial distribution in chord but operates as a segmented rotor with limited harmonic pitch. The final constraint is to interconnect each of the segments such that the twist variation radially will be characteristic of the first-mode torsion that can vary harmonically to provide the recommended rotor. The process starts with a Mangler loading (Reference 4) to minimize induced power, defines the "rubber chord and rubber twist," defines a weighted chord distribution that is then used in a comprehensive vortex theory forward flight analysis (B-65), and establishes an optimum twist. It is a sophisticated aerodynamic prediction technique that has as its starting point a uniform downwash rotor solution. From this solution, it then approximates the trailed vortex sheet by a number of vortices for the first 45 degrees of rotation; after that, it rolls up the tip vortex using the Betz loading criteria. It then calculates the nonuniform downwash and local aerodynamics at 13 radial stations and every 15 degrees around the azimuth. The output is the overall performance, radial, and azimuthal variations of all the characteristics of that rotor. Rotor elasticity in the first two flap modes and first torsion mode is accounted for. An examination is made of the chord and checked against the previous iteration. If there is a change in chord greater than 3 percent, then the process is repeated with the new thrust loading, induced-velocity distribution, and harmonic flapping coefficients and repeated until the tolerance in chord is achieved.

How good is the rotor performance prediction program? Here is an example of its predictive capability compared to wind tunnel test data from recent model tests. We tested a few model rotors to 230 knots in the wind tunnel and they had advanced airfoils and rectangular-tip blades and tapered-tip blades as described in Reference 3. Figure 6 is an example of how we

predict that model rotor in the high-speed regime (above 200 knots). Shown is rotor lift-to-equivalent drag ratio (L/De) versus advance ratio, which represents the lift and the power required to produce it, not including the propulsive power. The prediction is close to the model test data for the rectangular and the tapered-tip blade. This comparison was for a model of an advanced rotor. We are currently building a full-scale rotor and the way we estimate the full-scale performance from model rotor test data is to account for the Reynolds number effect on profile drag. When you scale up this model test data to full-scale by the procedure defined in Reference 5, you develop the L/De versus advance ratio presented in Figure 7. The maximum L/De is approximately 9 for a rotor with a solidity of 0.134. The comparison of theory, the black symbols, with test data, the open symbols and lines, is acceptable, being 7.5-percent pessimistic at 225 knots.

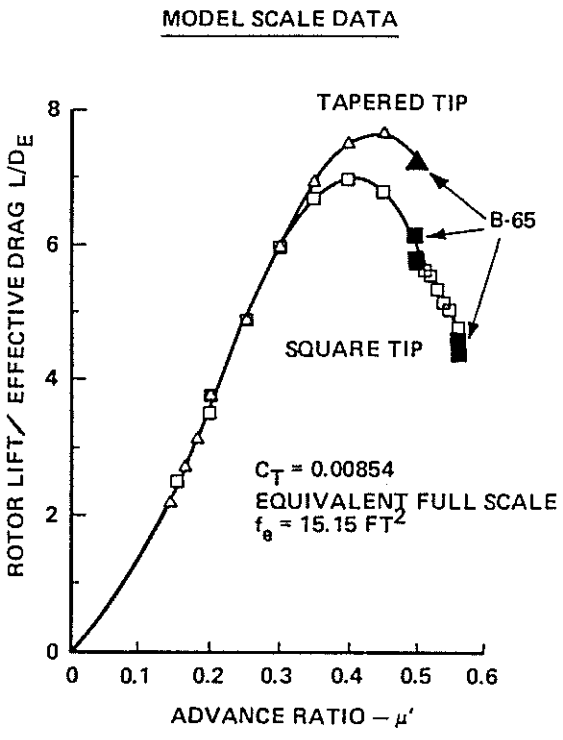

Figure 6. Comparison of Theory With Model Test Data

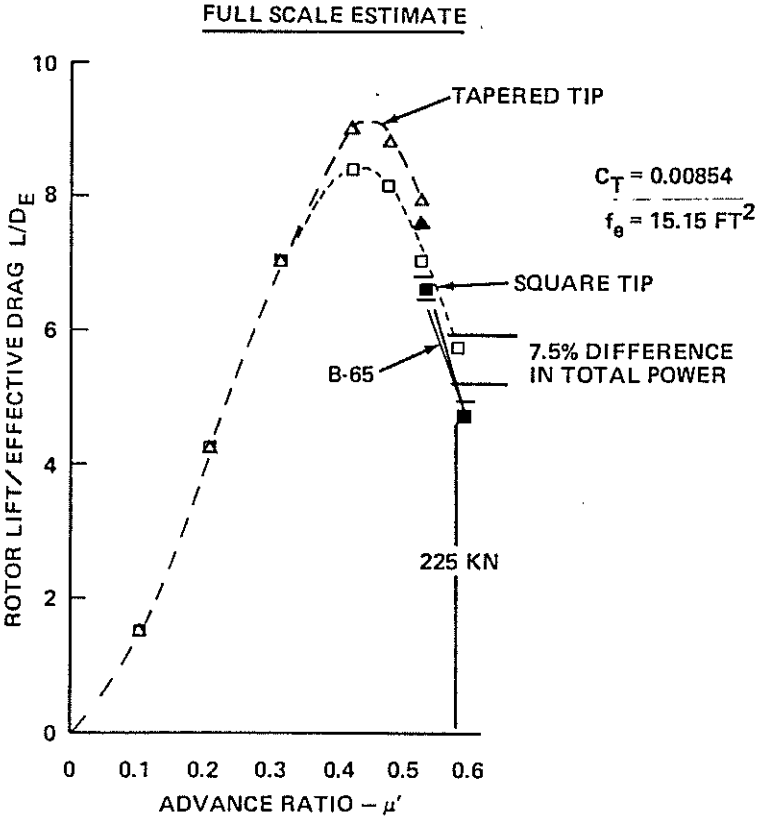

Figure 7. Comparison of Scaled-Up Model Test Data With Theory

We compare the performance prediction in this format because it relates lift with the power required to produce lift and expands any difference from the test data. If comparisons are made using C_P versus μ or C_T versus C_P at a fixed advance ratio, the comparison of theory could look fairly close, but the L/De could be 10 to 20 percent different. We are trying to get a better look at how good the analysis is and this format provides a relatively close look at it. The conclusion is that B-65 is a performance analysis that predicts performance quite well. It is a little conservative at 225 knots, about 7-percent pessimistic.

As indicated earlier, the reference rotor was the CH-46E rotor. It has a diameter of 51 feet, three blades with a chord of 1.5 feet, and 23010 airfoil constant from root to tip. Normal hover tip speed is 705 ft/sec, but an advancing-tip Mach number limit of 0.90 was imposed to be the same as the advanced rotor. The operating conditions selected are the same: gross weight = 25,000 pounds, which translates to a rotor lift coefficient (C_T/σ) of 0.0966 at 705 ft/sec; the propulsive force requirement is $\bar{X}$ = 0.056.

The performance of this rotor operating at a tip speed of 705 ft/sec for forward speeds up to 195 knots and then following a constant Mach number of 0.9 is presented in Figure 8. Power required is increasing very rapidly at speeds beyond 200 knots and the rotor system cannot operate beyond 215 knots. This is a result of stall and is reflected by the sharp break in the power required at 200 knots. Rotor stall is occurring on the forward and aft portions of the rotor as well as on the retreating side of the disk. The rotor lift-to-drag ratio (L/De) reaches a maximum of 7.0 at 150 knots and then decreases rapidly, approaching zero at 215 knots. That is an operational rotor designed and fabricated in the 1960's with 23010 airfoils. A rapid solution to the stall problem is to add another blade, going from a 3-bladed rotor to a 4-bladed rotor. The corresponding rotor performance is presented in Figure 8, indicating that rotor stall has been significantly reduced and the power required at 225 knots is 2,500 horsepower. This will be the level from which the advanced rotor performance improvement will be measured. The development of the advanced rotor will be described in the following sections.

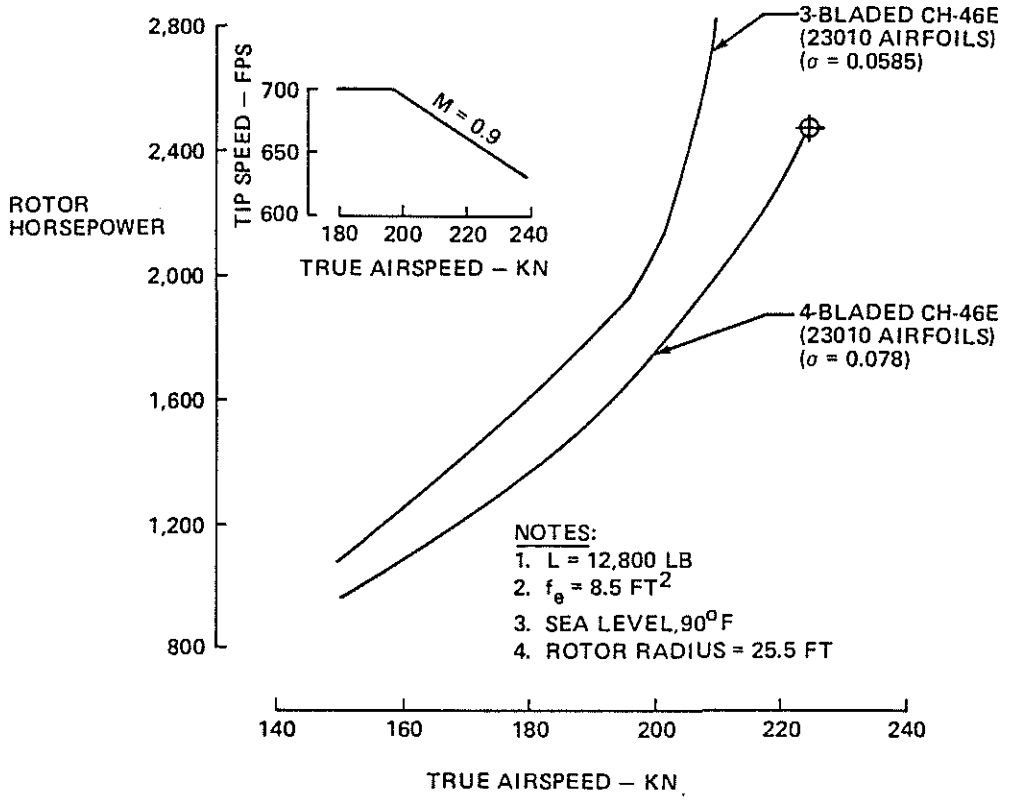

Figure 8. Performance of 3- and 4-Bladed Reference Rotor

7. IDEAL ROTOR

The process of defining the performance of the ideal rotor, depicted in Figure 9, was to define the lift coefficient (C_l) for maximum airfoil section lift-to-drag ratio (L/D) for each Mach number and then define the trend of L/D maximum with Mach number and operate each blade bay at the L/D to define minimum profile drag. A rotor pressure loading must be selected to provide the effectively uniform downwash in the far field to minimize induced drag. The Mangler 1 or the Mangler 3 loading both provide a uniform downwash in the far field. Combining both the requirements for minimum profile and induced drag will provide the rotor with minimum power required.

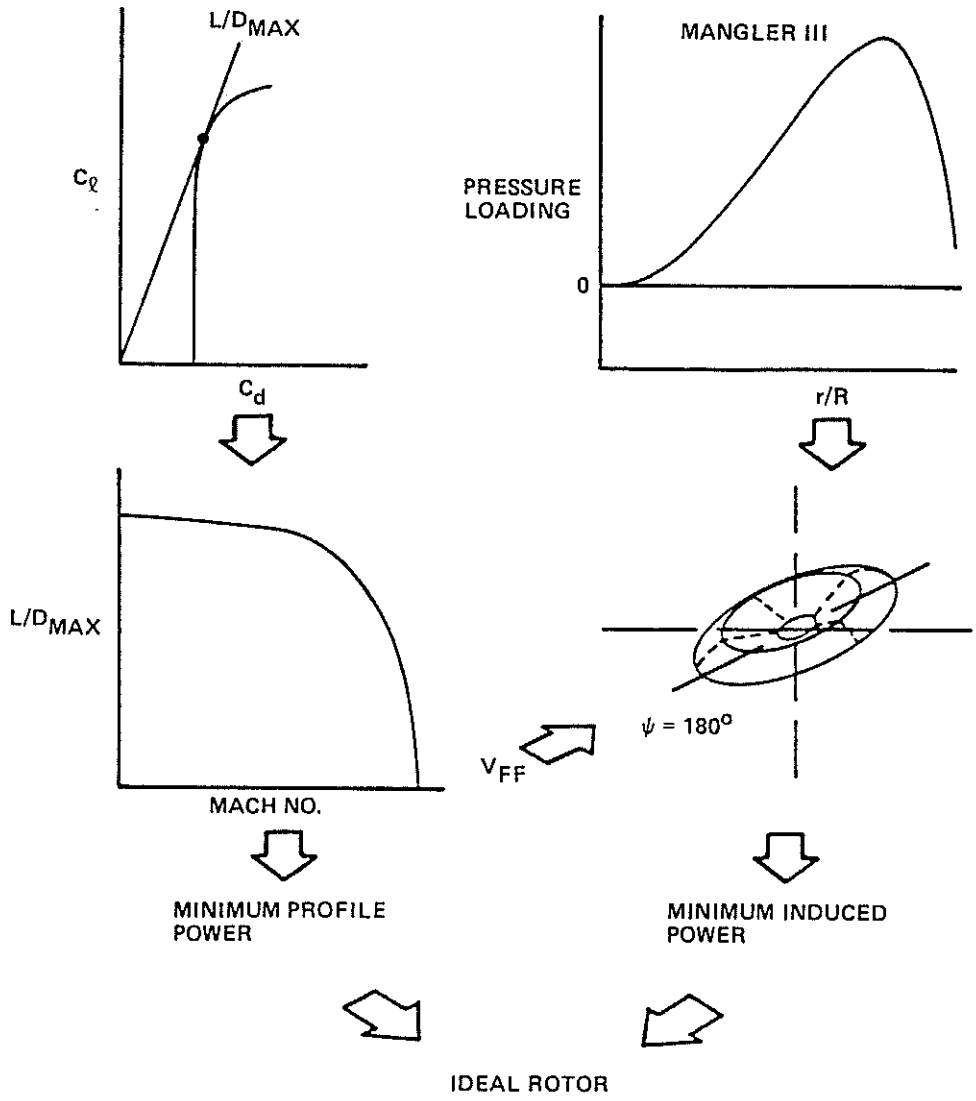

Figure 9. Performance Definition of Ideal Rotor

What is unique about Mangler 3? Why not Mangler 1? What is the sensitivity to either one of the loadings shown in Figure 10? They both provide uniform downwash in the far field. Mangler 1 is like an elliptically loaded wing. Mangler 3 is more like a hovering rotor. The performance associated with each loading is presented in Figure 11. In terms of power required, the Mangler 3 loading results in a power required of 1,600 hp. The Mangler 1 loading resulted in a lower power (1,440 hp). The induced power is basically the same but the change was in profile. Parasite power is the same since both loadings are flown at the same operating conditions. This resulted from the loading being reduced on the outboard end, loaded more on the inboard end of the advancing blade. Generating lift in the lower Mach number region instead of the higher Mach number region results in a higher section L/D, as shown in Figure 9. The change is a result of reducing the compressibility drag. If the compressibility is completely eliminated the power is reduced to approximately 1,250 hp. This quantifies the maximum potential but it is not obtainable. Rotor L/De is a measure of cruise efficiency and will be the format used in the remainder of the study; Mangler 3 had an L/De of approximately 16 while Mangler 1 was approximately 18. When the compressibility was removed the L/De increased to approximately 40, and when the profile power was removed the L/De became 85. The Mangler 1 loading will be used to evaluate the rotor development for the remainder of the study.

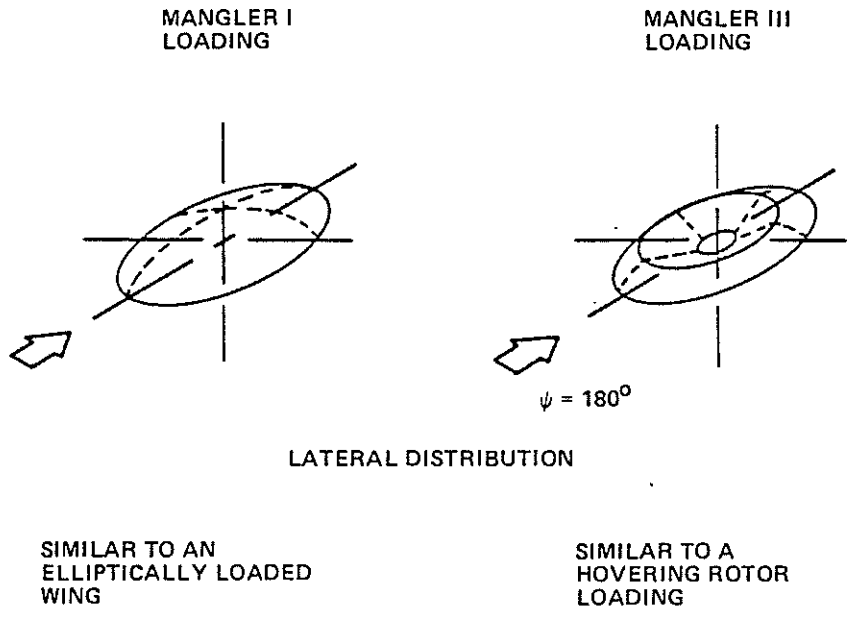

Figure 10. Loading of Ideal Rotor

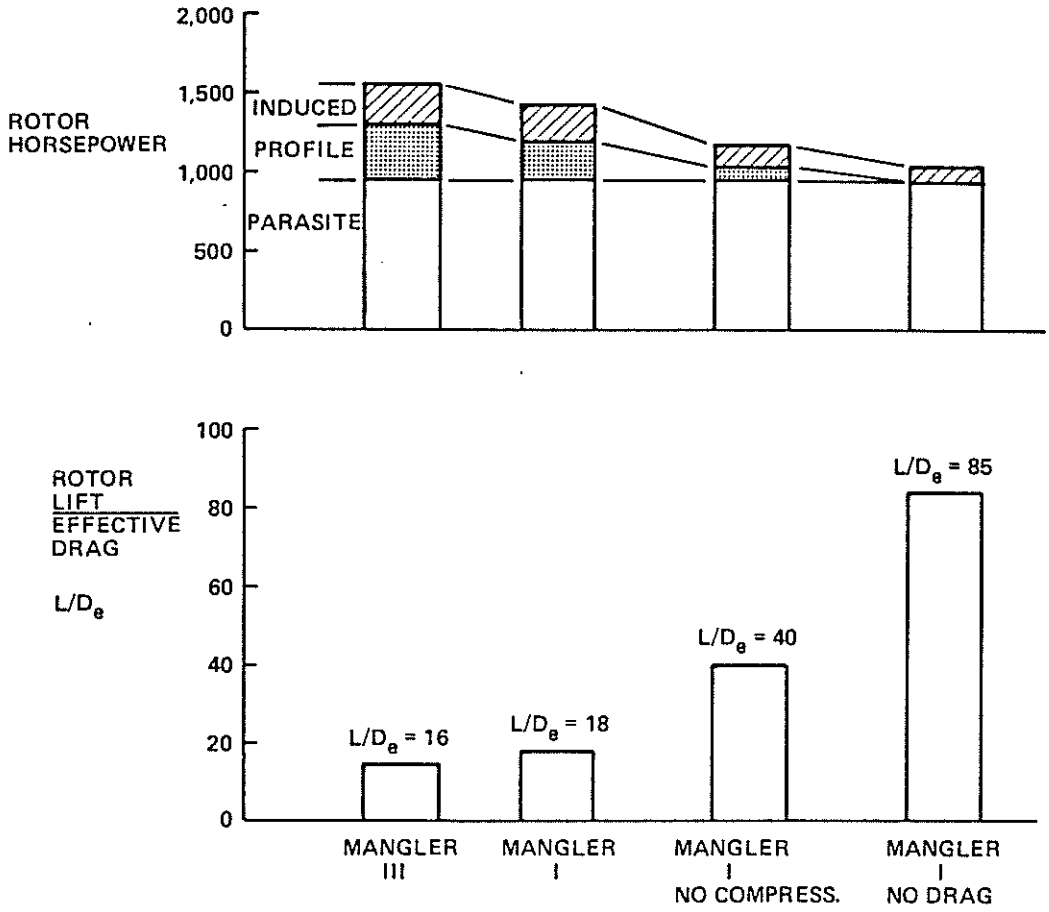

Figure 11. Sensitivity of Performance of Ideal Rotor to Loading

What are the effects of speed on this ideal rotor? Figure 12 presents the performance at 180, 200, and 225 knots, indicating that the profile grows slightly as speed increases to 200 knots but is virtually the same between 200 and 225 knots. The induced power grows just slightly. Parasite power has the largest power-required growth.

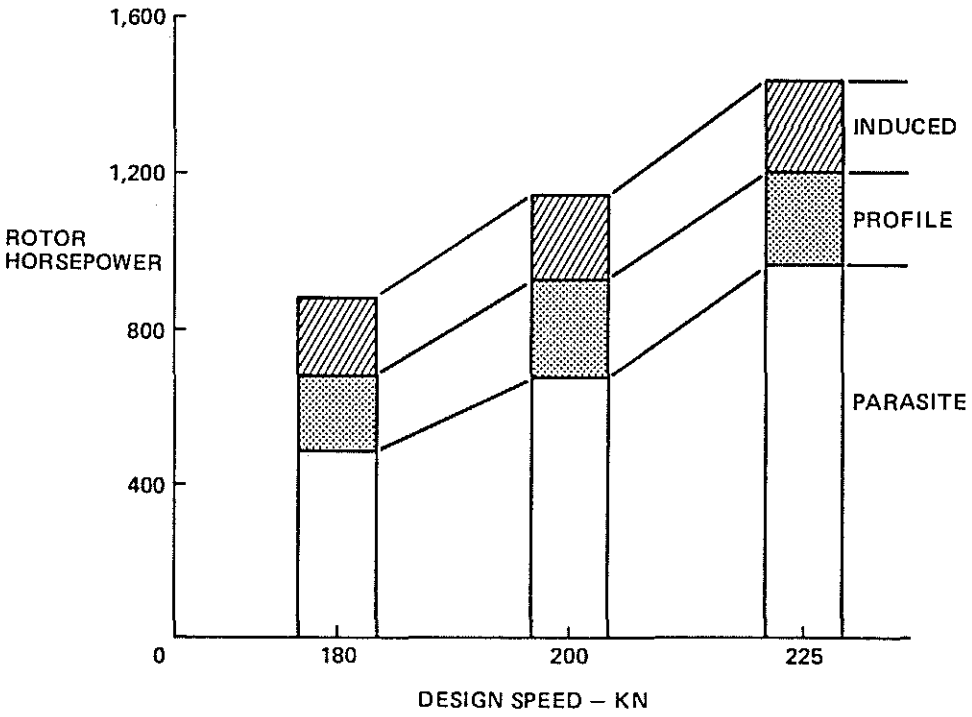

Figure 12. Sensitivity of Ideal Rotor to Design Speed

The design cycle was iterated a number of times to provide a loading, chord-twist distribution. It started off with a Mangler 1 loading and iterated four times to arrive at the final thrust loading. It is fore and aft loaded and the isometric view of the final thrust loading for the ideal rotor is presented in Figure 13.

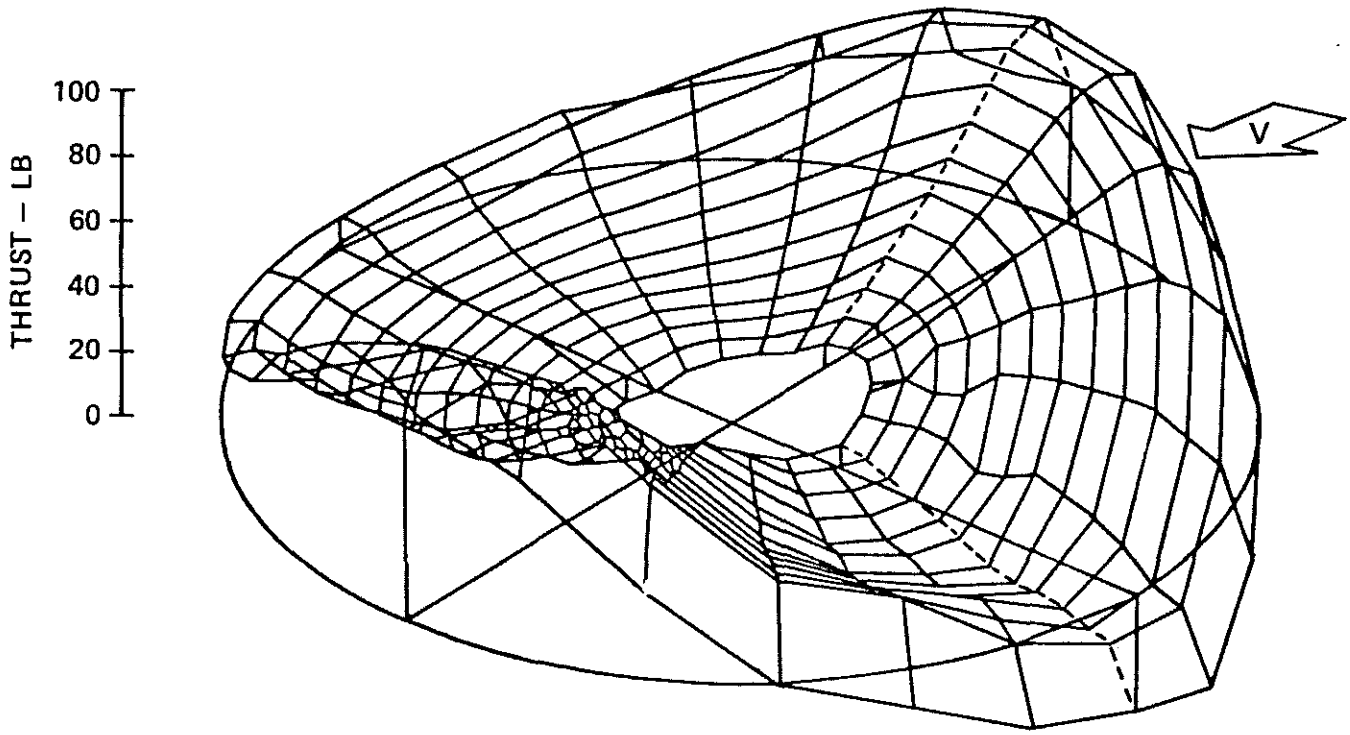

Figure 13. Final Thrust Loading for Ideal Rotor

8. OPTIMUM ROTOR

With the ideal rotor defined, the next step is to define the optimum rotor. The ideal rotor thrust loading and chord distribution, when presented as a surface plot and not as a radial distribution, look like the top of Figure 14. Combining the radial and azimuthal thrust and chord variation permits the definition of a thrust-weighted blade chord. The radial chord distribution, shown in Figure 14, is held at all azimuths and can then be used to establish the pitch requirements. This defines the optimum rotor with 13 bays, each one with a thrust-weighted chord that can operate at the pitch requirement shown in Figure 14. The blade chord was iterated through the design process a number of times and Figure 15 shows the chord distribution from each iteration, resulting in a chord distribution increasing radially to 2.2 feet at 88 percent of the blade radius and then decreasing to 1.4 feet at the blade tip. How do we know thrust-weighting the chord is the right way to do it? If you bias the chord toward the areas where you will have high thrust, is that right? Why not some other way? We are looking for maximum L/De, so why not bias the chord to that which provided the highest incremental rotor L/De for each blade segment? Much to our surprise, there was very little difference between the thrust-weighted and L/De-weighted chord. Utilizing the thrust-weighted chord, we are now ready to define the segmented rotor.

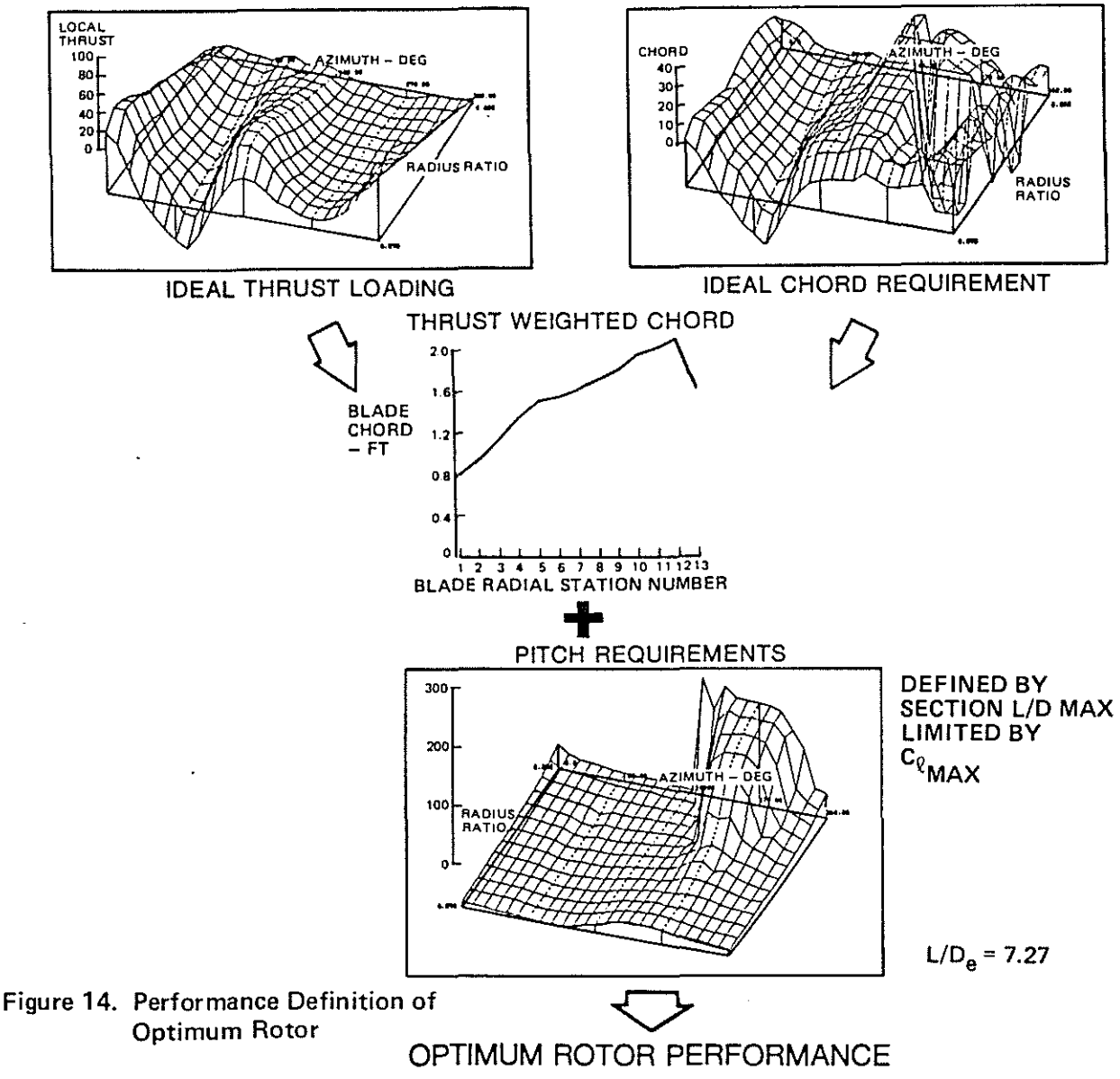

Figure 14. Performance Definition of Optimum Rotor

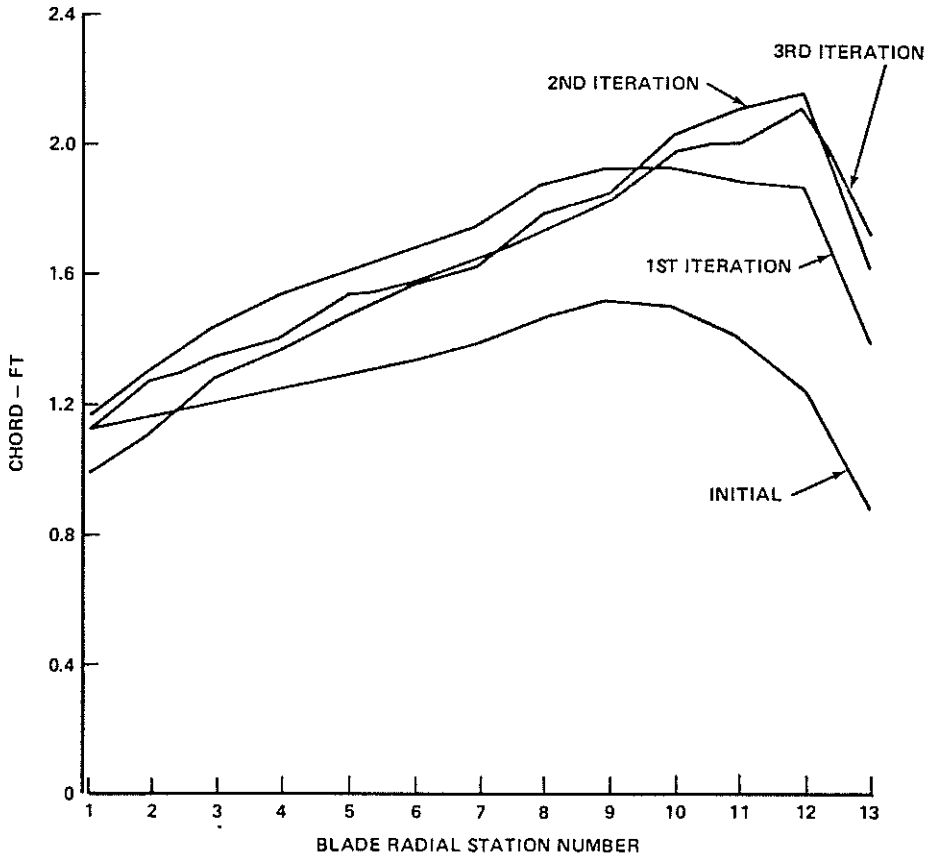

Figure 15. Iteration of Blade Chord for Optimum Rotor

9. SEGMENTED ROTOR

The segmented rotor is developed with the thrust-weighted chord and the optimum blade pitch shown in Figure 16. A harmonic representation of the optimum pitch is restricted to 0 through 5 harmonics as shown in Figure 16. It is important to point out that the fourth and fifth harmonics of the blade pitch are approximately zero. The pitch schedule for each segment of the blade when restricted to the steady plus the first 5 harmonics can be adjusted to provide the best approximation of the pitch (theta) schedule at all azimuths or on the advancing side of the rotor disk only. Examining both schedules to determine the impact on performance is summarized in Figure 17 with a comparison of the root and tip pitch variations around the azimuth. When the segment pitch approximated the optimum pitch at all azimuths, the rotor L/De was 6.73. When the segment pitch approximated the optimum pitch on the advancing side only, the L/De was 7.72. The optimum pitch has very large amounts of theta on the inboard end of the retreating blade. To get the harmonic fit at all azimuths and to provide this high pitch requirement results in a poor approximation of the pitch on the advancing side and degrades the performance. Providing the harmonic fit on the advancing side only results in a poor representation of the pitch on the retreating side of the rotor, but it does reduce the performance penalty on the advancing side. This provides a higher L/De and establishes the advancing side of the rotor disk as the area to which to carefully tailor the rotor definition and thereby minimize the negative lift and power penalty. This will be a guideline for the remainder of the study: match the pitch on the advancing side of the rotor only. Figure 18 presents a comparison of root and tip pitch for the optimum rotor with an L/De of 7.27, and for the segmented rotor meeting the pitch requirements on the advancing side having an L/De of 7.72. All of these comparisons were made at 225 knots with the rotor in trim with flapping minimized.

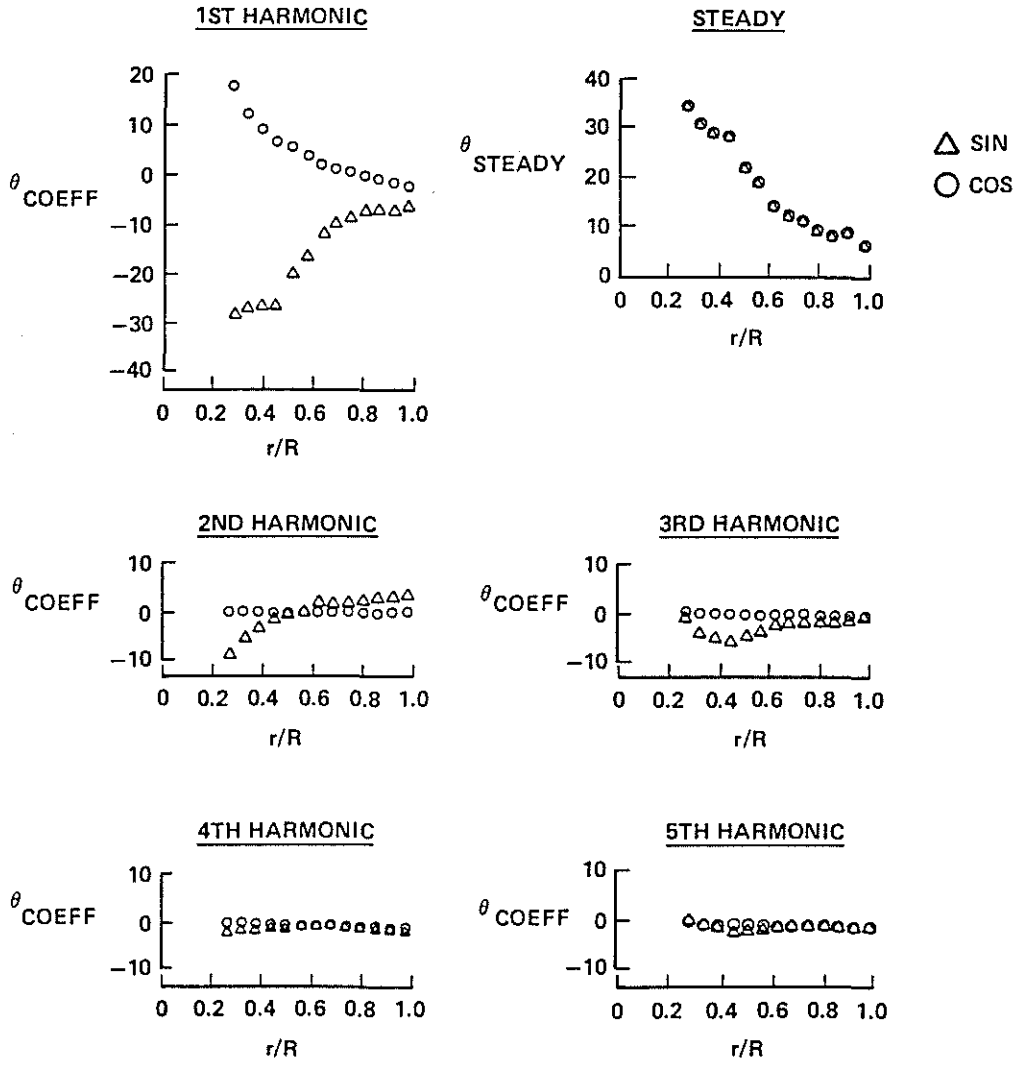

Figure 16. Harmonics of Pitch Distribution of Optimum Rotor

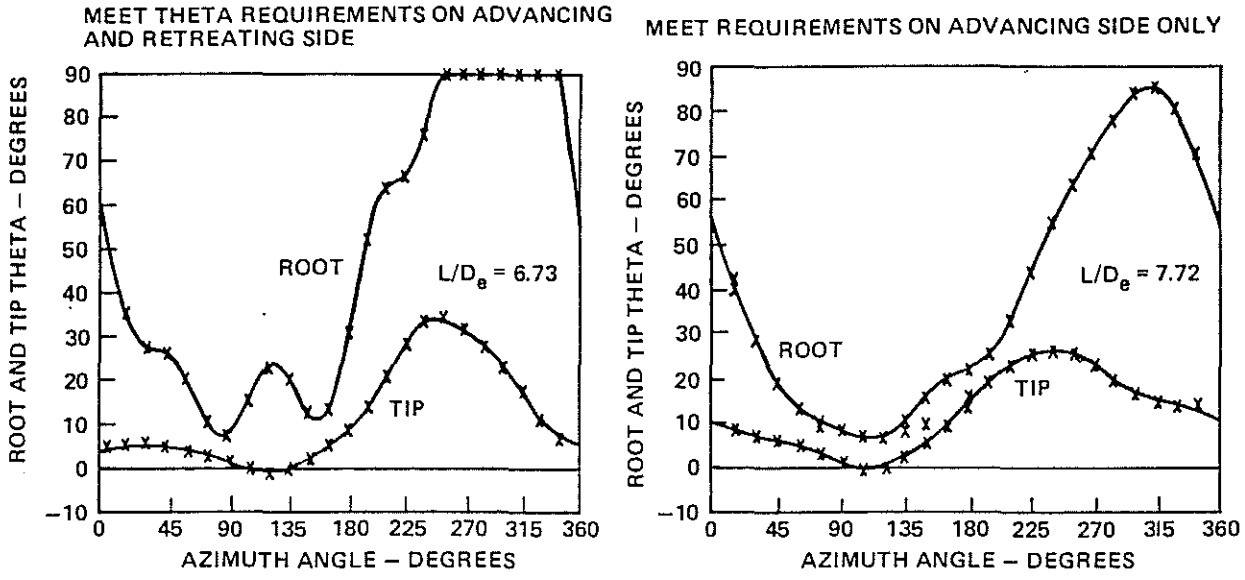

Figure 17. Impact of Pitch Schedule on Performance of Segmented Rotor

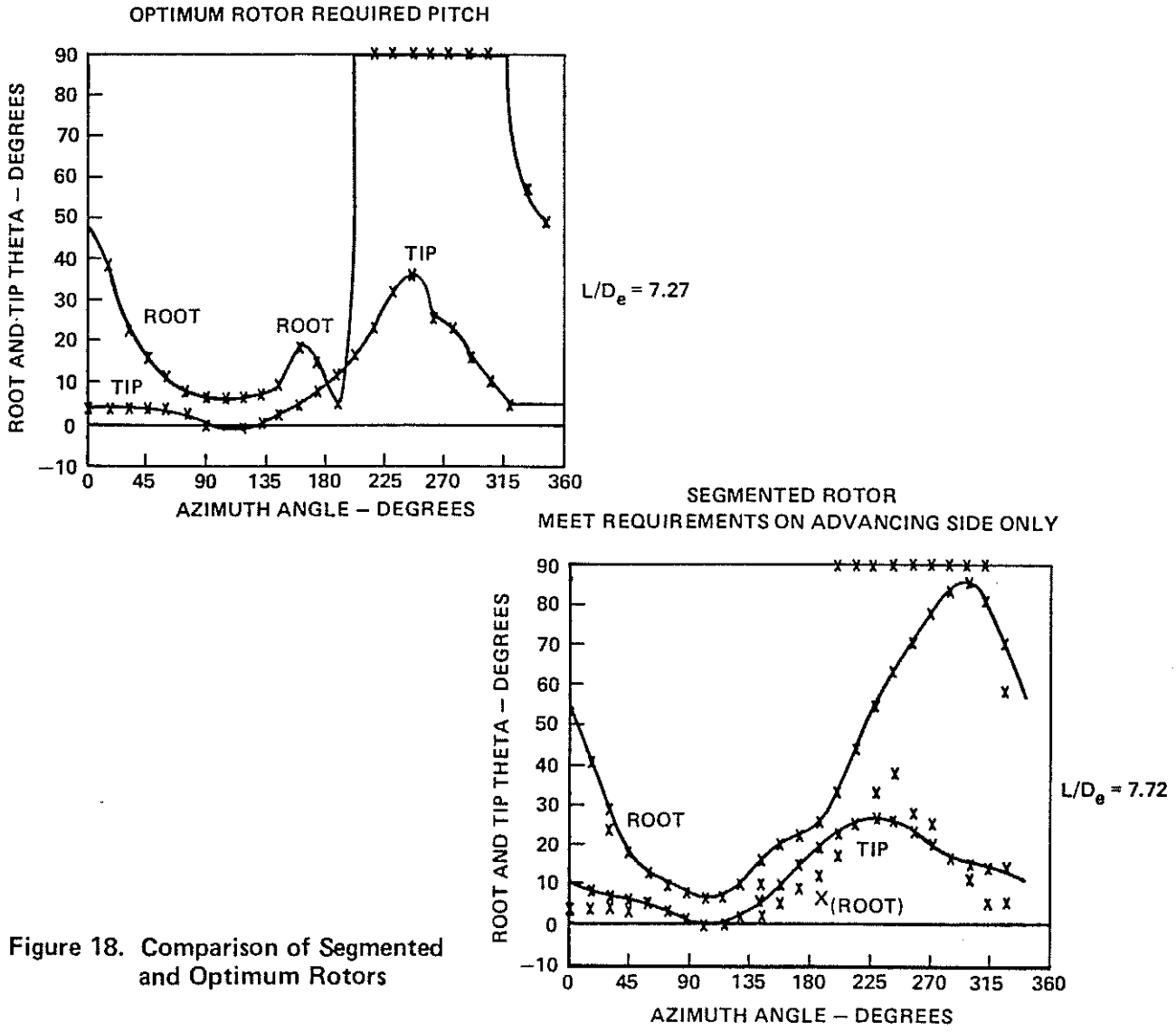

Figure 18. Comparison of Segmented and Optimum Rotors

10. RECOMMENDED ROTOR

The next step in the rotor development is to constrain the twist radially to the first-torsion-mode shape that typically looks like the top of Figure 19. Also shown in Figure 19 are the first and second harmonic thetas, represented by the symbols, with the lines representing the best fit to the torsion mode shape. Now a fit with many of the thetas, or a few of them, can be achieved, but which ones should be fit to achieve the best performance? A study was performed to determine what portion of the blade should be matched to a first-torsion-mode shape. Figure 20 presents the highlights in terms of root and tip pitch and L/De for the specified-twist rotor and should be compared to Figure 18, the segmented rotor with an L/De of 7.72. When the first-torsion-mode shape was matched to the thetas over the outboard 50 percent of the blade, the rotor L/De was 8.41. The tip pitch looks approximately the same as the segmented rotor and the root pitch is similar except in the second quadrant. When a match was achieved over the outboard 40 percent, the L/De increased slightly to 8.63. The root pitch in the fourth quadrant is lower than the 50-percent case. Matching only the outboard 35 percent, the rotor L/De dropped to 8.35 and the root pitch has increased in the fourth quadrant. The conclusion is to match the pitch requirements to the outboard 40 percent on the advancing side of the rotor disk. This results in an elastic twist requirement of 18 degrees.

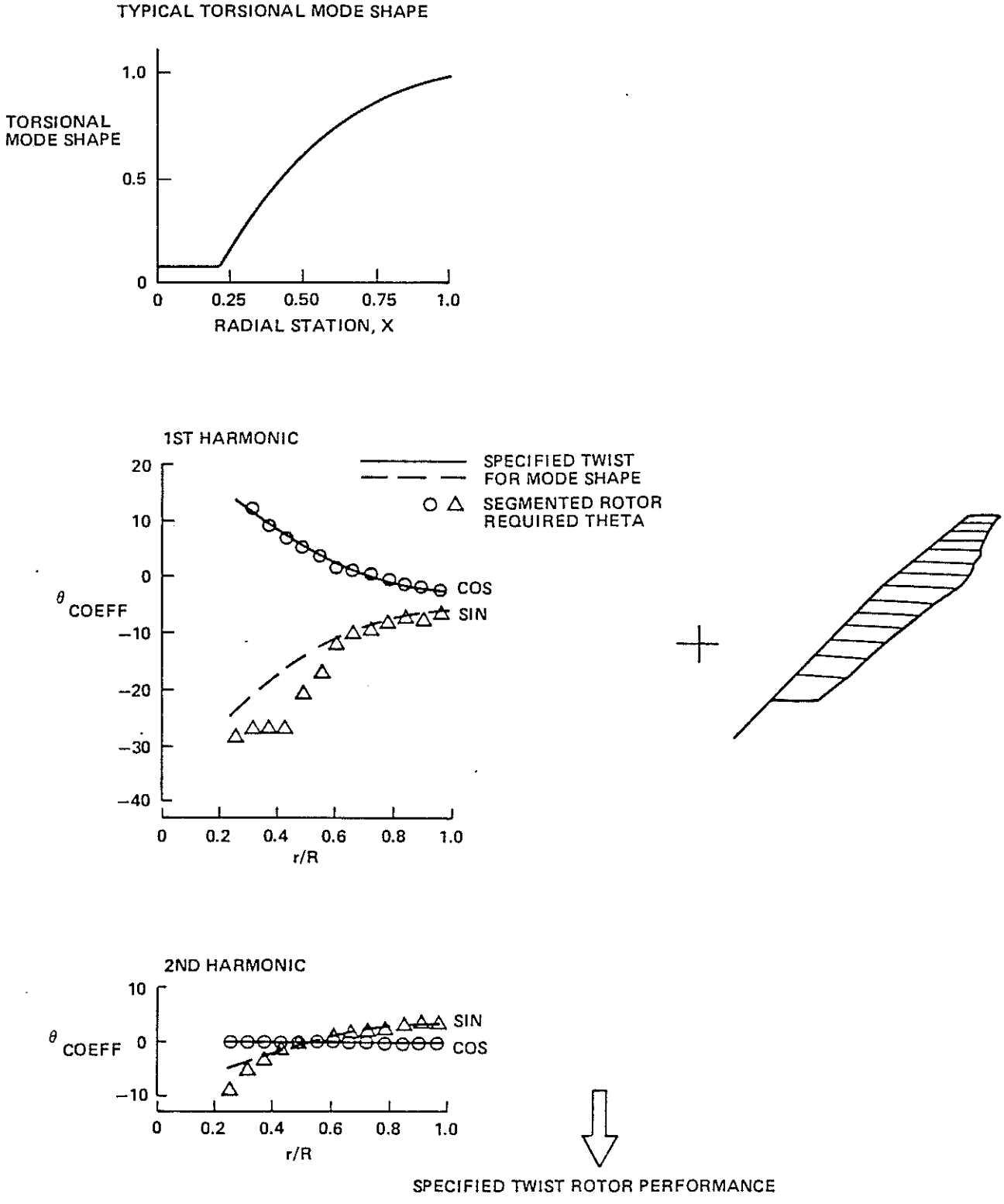

Figure 19. Definition of Specified Twist Rotor

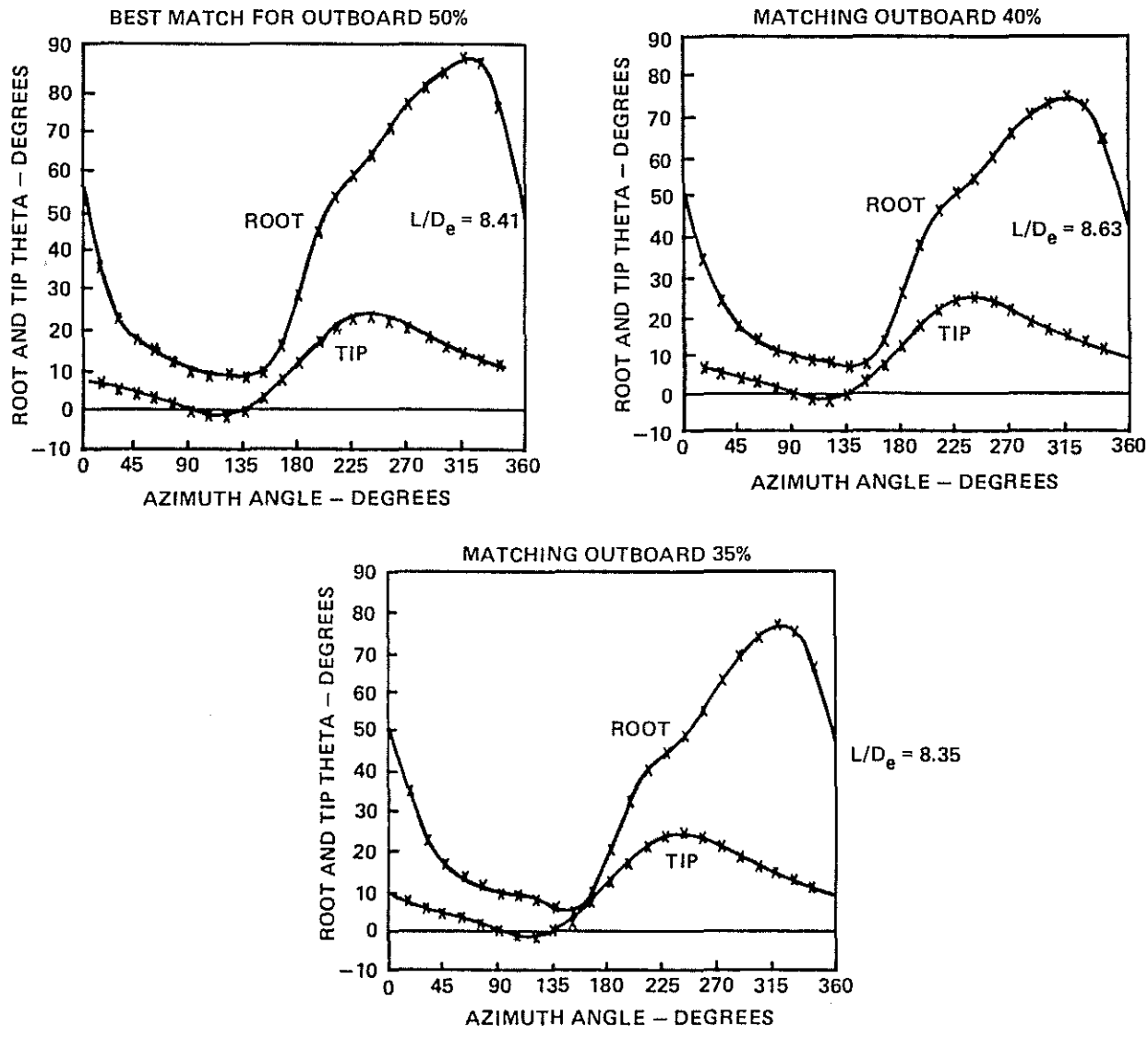

Figure 20. Performance and Blade Pitch of Specified-Twist Rotor

Having defined a blade planform and a static and elastic twist, we conducted sensitivity studies on planform, blade stiffness on the inboard end (basically to reduce elastic twist), and the radial distribution of airfoils.

Sensitivity to Planform

The basic planform shown at the top of Figure 21 has an inverse taper from the root to 88 percent of the rotor radius and conventional taper to the tip, with an L/De of 8.63. This is the configuration on which we determined the sensitivities. The approach was to gradually step back to a blade that is rectangular. The first step was to reduce the taper on the inboard end halfway back to no taper, as shown by the dotted lines. The L/De falls off just slightly. With no inboard taper the L/De decreases from 8.63 to 8.25. When reducing the taper on the outboard end all the way to a rectangular blade there is no further reduction in L/De for the prescribed pitch distribution.

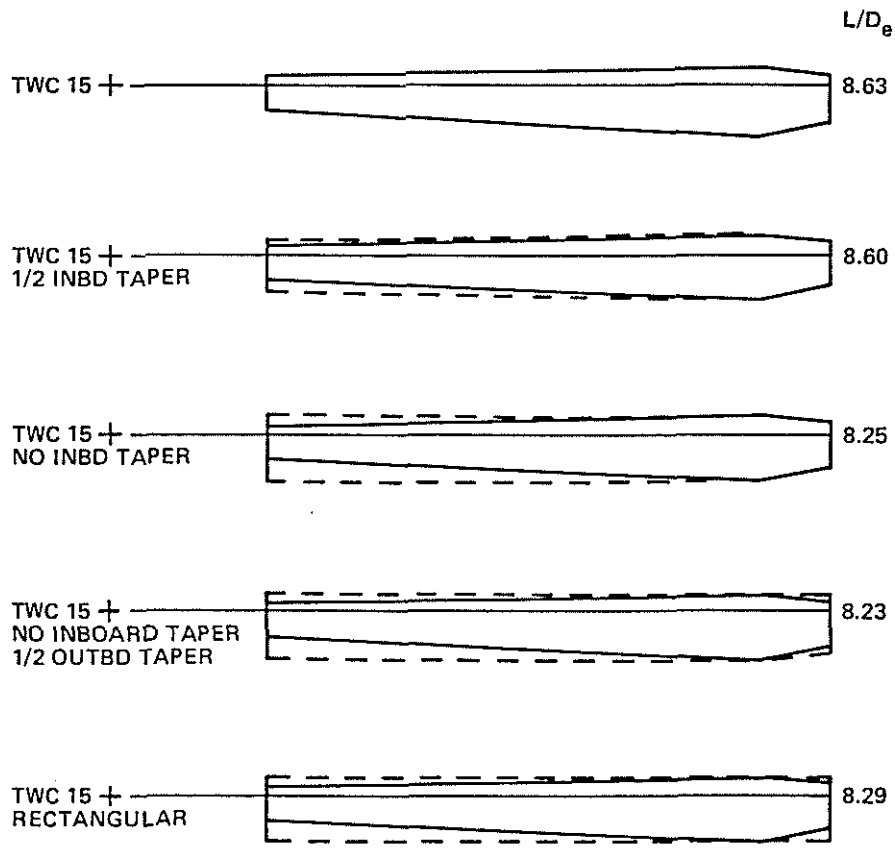

NOTE: ALL TWIST SCHEDULES IDENTICAL

Figure 21. Sensitivity Study of Planform

Sensitivity to Blade Stiffness on the Inboard End

The torsional mode shape shown in Figure 19 indicated a high level of stiffness out to the blade attachment in the basic design. In the blade development we had matched the twist to the torsion mode shape on the outboard portion of the blade as shown in Figure 20; the remainder of the blade had an elastic twist requirement greater than the mode shape. When the blade is stiffened on the inboard end the elastic twist requirements could be reduced. If the elastic twist could be reduced without a performance penalty, it would simplify the structural design problem. The sensitivity study examined increasing stiffness of the blade out to 40, 50, 60, and 70 percent of the span, as shown at the top of Figure 22. The impact of inboard stiffness on elastic twist requirements is shown in the middle of Figure 22. The baseline blade has an elastic twist of 18 degrees at 90 degrees rotor azimuth; when the blade was stiffened to 40 percent, that drops to approximately 12 degrees. As the stiffness is increased to 50, 60, and 70 percent, the elastic twist correspondingly reduces to 9, 5, and 3 degrees. What is happening to L/De or power required? The bottom of Figure 22 shows power required reducing gradually as the stiffness is increased outboard and the L/De, which magnifies the difference in performance, gradually increasing from 8.63 for the baseline to 8.73 for a blade stiffened out to 60 percent. Stiffening to 70 percent results in a very slight reduction in L/De. As indicated earlier, matching the elastic twist from 60-percent radius to the tip maximizes the rotor performance and stiffening the blade inboard of 60 percent reduces the elastic twist significantly; in addition, it provides an additional slight improvement in rotor L/De. When the blade is stiffened in this manner not only are the elastic twist requirements changed but also the steady geometric twist definition

must change to compensate for the new steady elastic twist level. To demonstrate the changes in elastic twist, a comparison of the baseline twist requirements was made with those of the blade stiffened out to 60 percent. Our baseline, the specified-twist rotor, had a steady geometric plus elastic twist variation as presented at the top of Figure 23. Stiffening out to 60 percent significantly reduced the requirement for what is built in the blade. In the center of Figure 23 is the azimuthal variation in the tip pitch and root pitch for the specified-twist rotor represented by the solid lines. The impact of stiffening drastically reduced the root pitch in the third and fourth quadrants of the rotor and had no effect on the tip pitch. Subtracting the difference between the root and the tip defines the elastic twist shown at the bottom of Figure 23. The solid line represents the baseline and the dashed line represents the increased inboard stiffness.

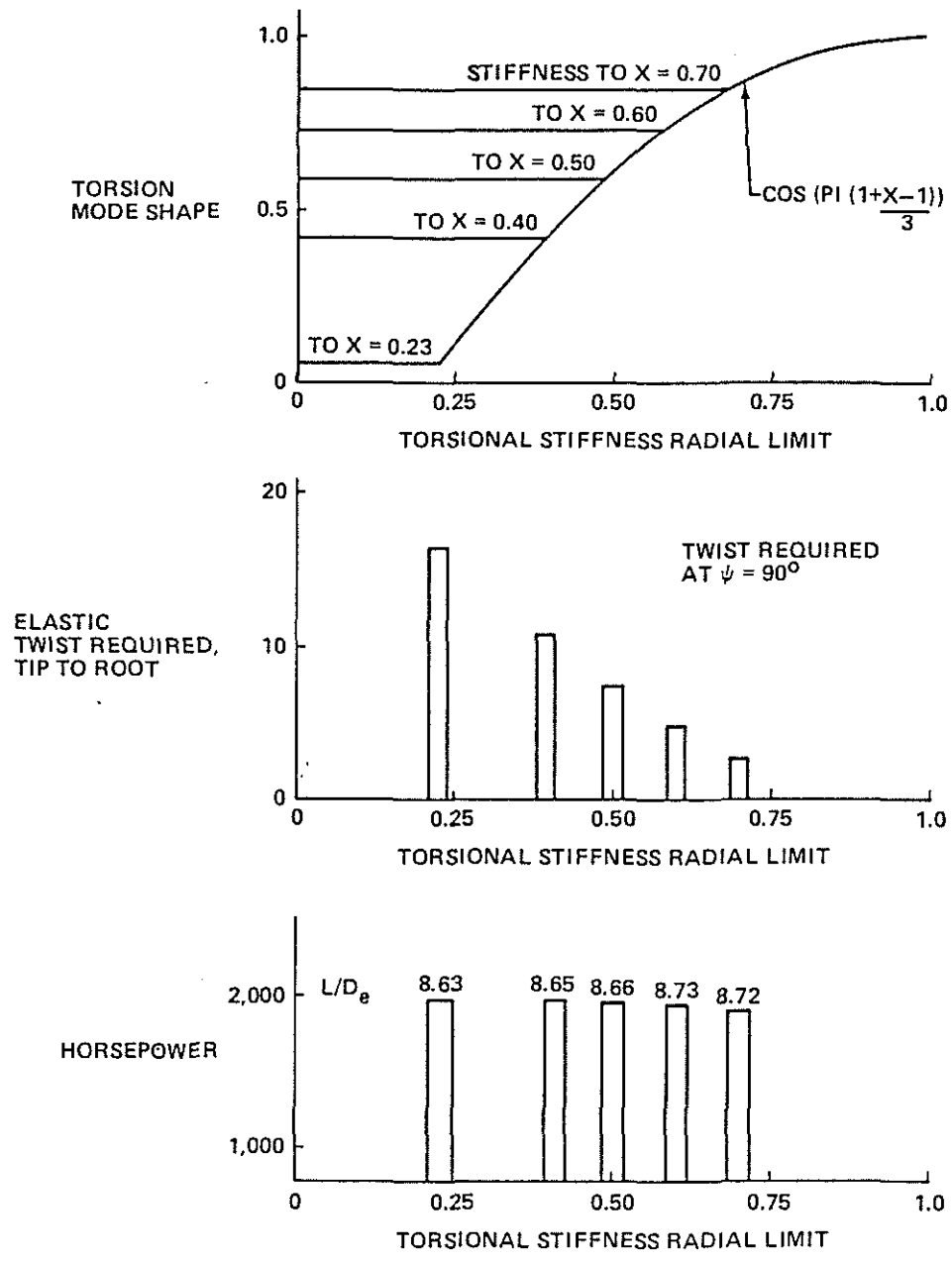

Figure 22. Sensitivity Study of Inboard Blade Stiffness

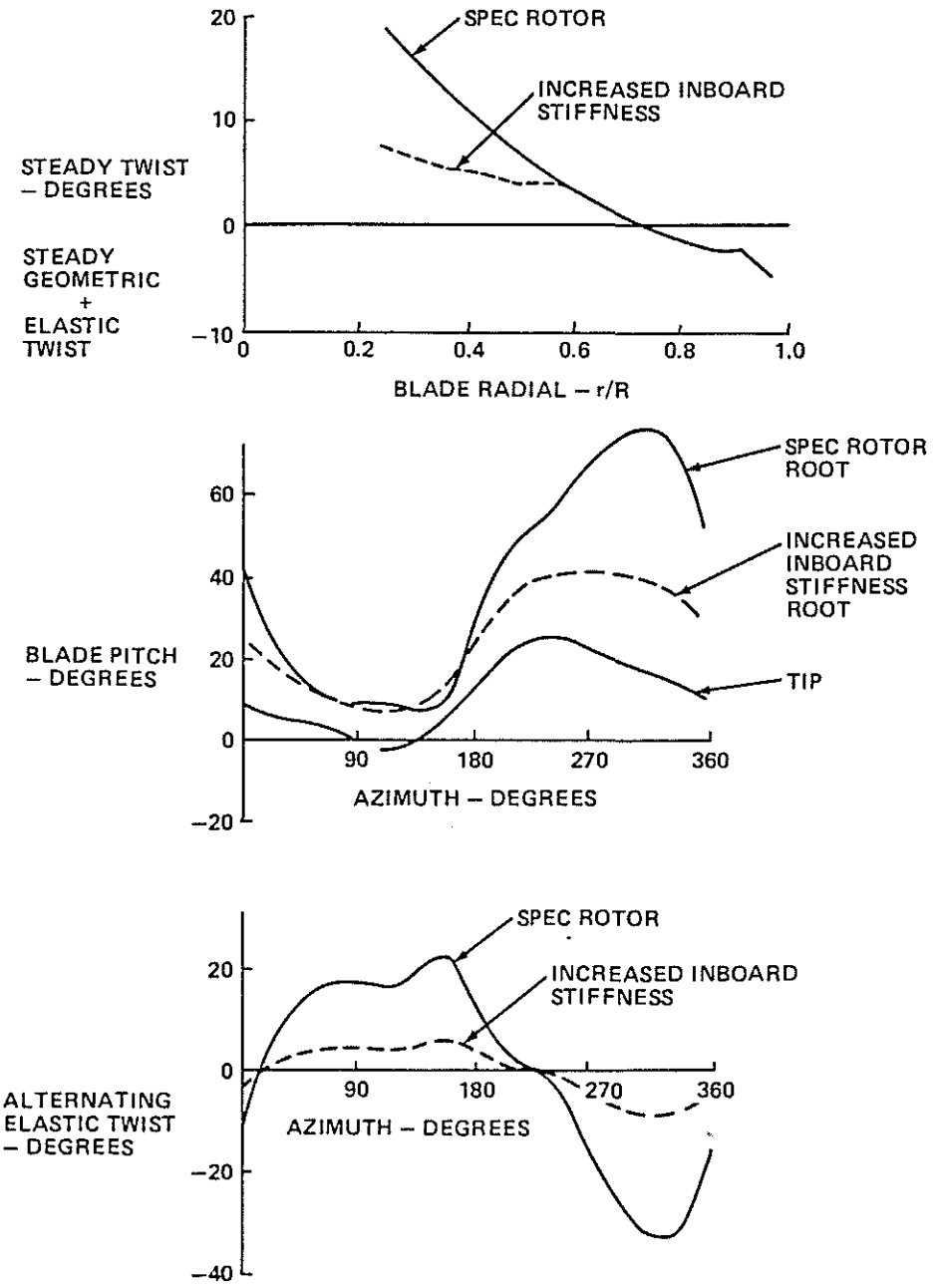

Figure 23. Effect of Inboard Stiffness on Blade Twist Requirements

Sensitivity to Airfoil Distribution

The baseline blade incorporates the VR-12 airfoil from the blade root to 85-percent radius, tapering to VR-15 over the last 15 percent of the blade radius. A sensitivity study was conducted to determine if this distribution provided the maximum performance. The VR-12 airfoil was extended from the root to the blade tip and the L/De decreased from the baseline as indicated in Figure 24. As the span of the VR-12 was reduced from the baseline, the 15-percent radial span for transitioning from the VR-12 to the VR-15 was held constant and the remainder of the blade was a constant VR-15. The rotor L/De increases as the span of the VR-12 is reduced to 75 percent and then the L/De decreases rapidly as the span is reduced to the blade root. Maximum performance is achieved with the VR-15 on the last 10 percent of the blade and provides the improvement through reducing compressibility power.

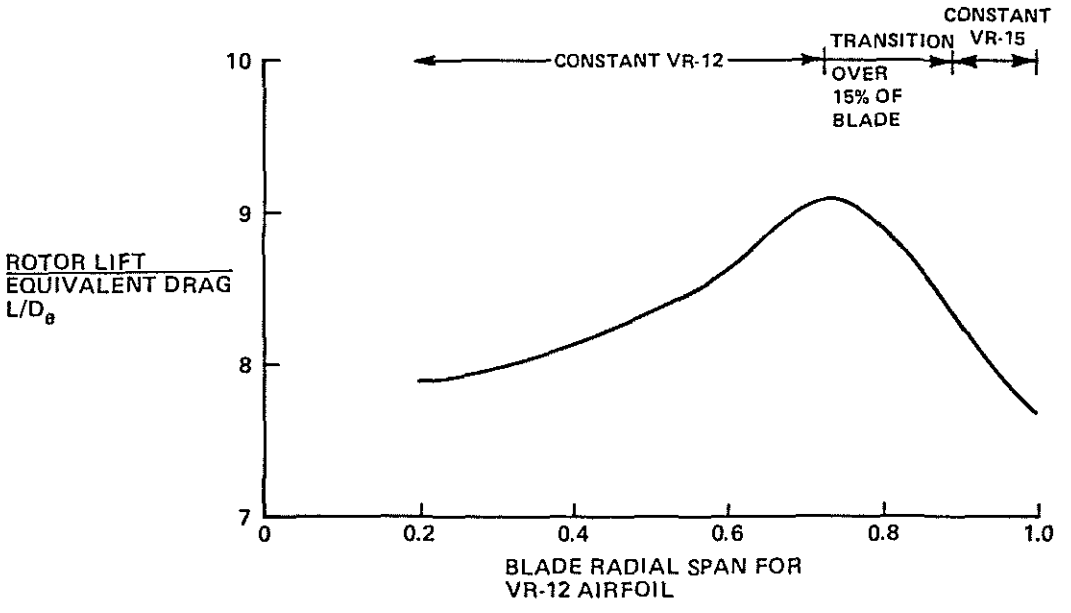

Figure 24. Sensitivity Study of Airfoil Distribution

For the blade developed in this program, a study was conducted to determine the feasibility of defining a blade to meet these requirements. The Model 360 rotor which is the advanced rotor we have been working on for the past few years served as the starting point. The characteristics were scaled down as the chord varied and a structural ply layup was established to match these characteristics. Figure 25 is the initial ply layup defining the distribution between graphite, fiberglass and Nomex honeycomb. This layup is not significantly different from that of the Model 360 and indicates that the blade is feasible.

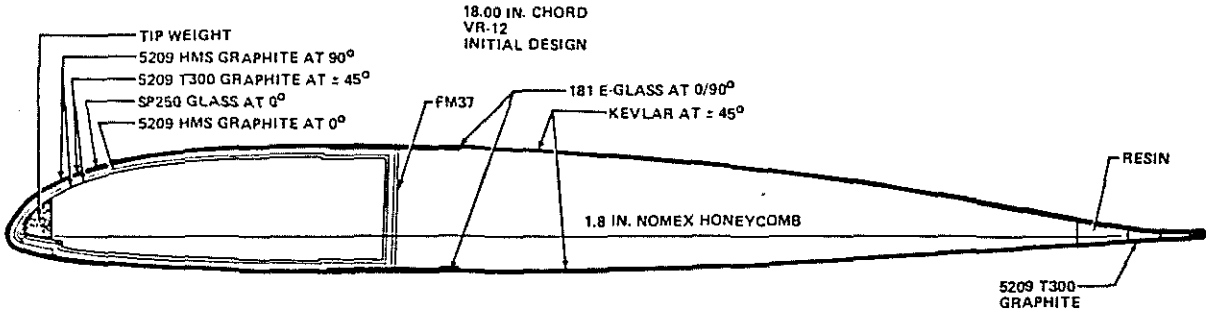

Figure 25. Initial Composite Ply Layup for Recommended Blade

How do we stack up against the reference rotor? Figure 26 presents the power required versus speed for the reference rotor. Shown in Figure 26 is the recommended rotor that is stiffened out to 60 percent and the power required is approximately 1,900 horsepower; the L/De is 9.1, a 60-percent improvement. How far did we get toward our ideal? Starting from the reference rotor, the reduction in power was 60 percent of the savings provided by the ideal rotor with a Mangler 1 loading.

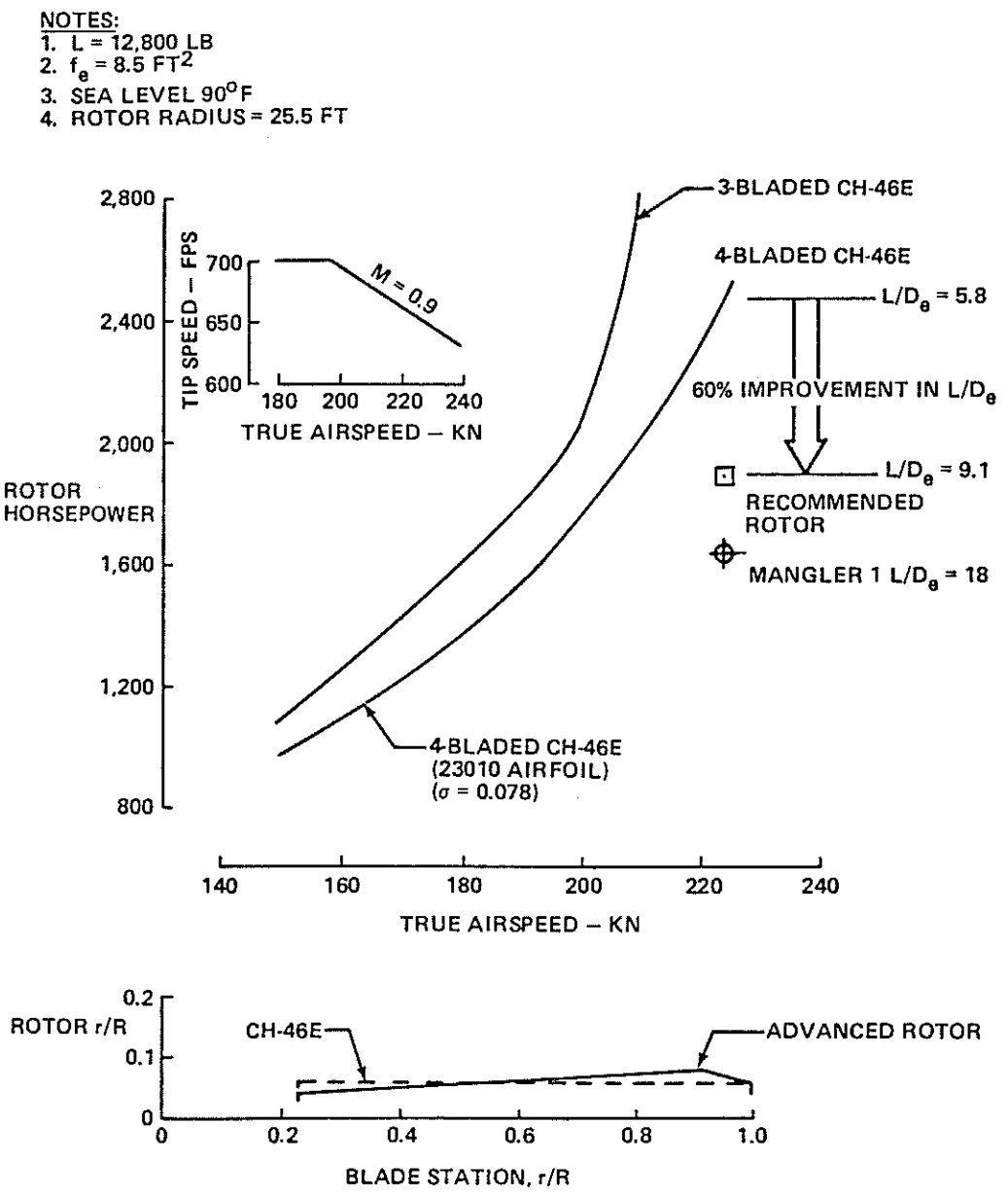

Figure 26. Results of Preliminary Study

11. CONCLUSIONS

In designing the rotor for 225 knots to achieve maximum performance, the following conclusions have been developed:

- Initiate the development process using the Mangler 1 loading and operate the airfoils at maximum section L/D.

- Use a prediction technique that incorporates nonuniform inflow and a comprehensive wake model and trim the rotor flapping to approximately zero to be most representative of the actual rotor operating conditions.

- Use thrust weighting to define the blade chord.

- The recommended blade planform has an inverse taper to 88 percent and conventional taper to the tip, providing the maximum rotor L/De.

- The elastic twist is basically first and second harmonic with a very small amount of third harmonic.

- It is mandatory to match the optimum pitch on the advancing side of the rotor to maximize performance.

- Inboard stiffness reduces the twist requirement and improves rotor L/De.

The next step is now funded by NASA to define the combination of design parameters that will aid in achieving the required pitch and twist.

12. ACKNOWLEDGMENTS

Many people have contributed to the development of the data and understanding presented in this paper. I would like to thank Len Haslim of NASA Ames, the technical monitor. I would also like to thank Hal Rosenstein, Doug Julian, Roger Lacy, and Kaydon Stanzione of Boeing Vertol who contributed directly and most significantly to the methodology, understanding, and data presented herein.

13. REFERENCES

1. McHugh, Frank J., and Harris, Franklin D., HAVE WE OVERLOOKED THE FULL POTENTIAL OF THE CONVENTIONAL ROTOR?, Journal of the American Helicopter Society, Washington, DC, July 1976.

2. McHugh, Frank J., WHAT ARE THE LIFT AND PROPULSIVE FORCE LIMITS AT HIGH SPEED FOR THE CONVENTIONAL ROTOR? Preprint No. 78-2, presented at The 34th Annual National Forum of the American Helicopter Society, Washington, DC, May 1978.

3. McVeigh, M. A., and McHugh, Frank J., RECENT ADVANCES IN ROTOR TECHNOLOGY AT BOEING VERTOL, Preprint No. A-82-38-03-0000, presented at The 38th Annual National Forum of the American Helicopter Society, Anaheim, CA, May 1982.

4. Mangler, K. W., CALCULATION OF THE INDUCED VELOCITY FIELD OF A ROTOR, RAE Report Aero 2247, Royal Aircraft Establishment, Farnborough, England, February 1948.

5. Keys, Charles N., McVeigh, M. A., Dadone, Leo, and McHugh, F. J., CONSIDERATIONS IN THE ESTIMATION OF FULL-SCALE ROTOR PERFORMANCE FROM MODEL ROTOR TEST DATA, presented at The 39th Annual National Forum of the American Helicopter Society, St. Louis, MO, May 1983.